

# Freezing Rogue Waves by Quantum Zeno Dynamics

Cihan Bayındır<sup>1</sup> and Fatih Ozaydin<sup>2</sup>

<sup>1</sup>Engineering Faculty, Işık University, İstanbul, Turkey.

Email: cihan.bayindir@isikun.edu.tr

<sup>2</sup>Faculty of Arts and Sciences, Işık University, İstanbul, Turkey.

We investigate the quantum Zeno dynamics of the rogue waves that are encountered in optics and quantum mechanics. Considering their usage in modeling rogue wave dynamics, we analyze the quantum Zeno dynamics of the Akhmediev breathers, Peregrine and Akhmediev-Peregrine soliton solutions of the nonlinear Schrödinger equation. We show that frequent measurements of the wave inhibits its movement in the observation domain for each of these solutions. We analyze the spectra of the rogue waves under Zeno dynamics. We also analyze the effect of observation frequency on the rogue wave profile and on the probability of lingering of the wave in the observation domain.

PACS numbers: 03.65.Xp, 03.65.Ta, 42.25.-p, 42.65.Tg

## I. INTRODUCTION

Rogue (freak) waves can be described as high amplitude waves with a height bigger than 2 – 2.2 times the significant waveheight in a wavefield. Their studies have become extensive in recent years [1–4]. The research has emerged with the investigation of one of the simplest nonlinear models, which is the nonlinear Schrödinger equation (NLSE)[1]. Discovery of the unexpected rogue wave solutions of the NLSE resulted in seminal studies of rogue wave dynamics, such as [1]. Their existence is not necessarily restricted to optical media [5], they can also be observed in hydrodynamics, Bose-Einstein condensation, acoustics and finance, just to name a few [1, 2]. It is natural to expect that in a medium whose dynamics are described by the NLSE and NLSE like equations, rogue waves can also emerge.

Analyzing the dynamics, shapes and statistics of rogue wavy optical fields are crucially important to satisfy certain power and communication constraints. Considering that the light can be quantized and the dynamics of atomic particles can be described by the NLSE, it is natural to expect that rogue waves can also be observed in quantum mechanical systems. In this study we consider the rogue waves encountered in optics and in quantum mechanics, for latter the ‘rogue wavefunction’ terminology can also be used.

On the other hand, Zeno dynamics [6, 7], which is the inhibition of the evolution of an unstable quantum state by appropriate frequent observations during a time interval has attracted an intense attention in quantum science, usually for protecting the quantum system from decaying due to inevitable interactions with its environment. It emerged that the observation alters the evolution of an atomic particle, even can stop it [8–10]. Duan and Guo showed that the dissipation of two particles can be prevented [11, 12], Viola and Lloyd proposed a dynamical suppression of decoherence of qubit systems [13], Maniscalco et al. proposed a strategy to fight against the decoherence of the entanglement of two atoms in a lossy resonator [14], Nourmandipour et al. studied Zeno and

anti-Zeno effects on the entanglement dynamics of dissipative qubits coupled to a common bath [15], and Bernu et al. froze the coherent field growth in a cavity [16].

Quantum Zeno dynamics can also be used for creating entanglement and realizing controlled operations. Wang et al. proposed a collective threshold measurement scheme for creating entanglement, avoiding the difficulty of applying CNOT gates or performing Bell measurements [17], which can be extended to multipartite entangled states. Since the generation of W states is more sophisticated than the generation of GHZ states or cluster states [18–22], Chen et al. proposed to use Zeno dynamics for generation of W states robust against decoherence and photon loss [23] and Barontini et al. experimentally demonstrated the deterministic generation of W states by quantum Zeno dynamics [24]. Nakazoto et al. further showed that purifying quantum systems is possible via Zeno-like measurements [25]. Classical analogues of quantum Zeno dynamics have also been reported in optical fibers [26–28].

In this paper we numerically investigate the quantum Zeno dynamics of the rogue waves that are encountered in optics and quantum mechanics. With this motivation, in the second section of this paper we review the NLSE and the split-step Fourier method for its numerical solution. We also review a procedure applied to wavefunction to model the Zeno dynamics of an observed system. In the third section of this paper, we analyze the quantum Zeno dynamics of the Akhmediev breathers, Peregrine and Akhmediev-Peregrine soliton solutions of the NLSE, which are used as models to describe the rogue waves. We show that frequent measurements of the wave inhibits the movement of the wave in the observation domain for each of these types of rogue waves. We also analyze the spectra of the rogue waves under Zeno dynamics and discuss the effect of observation frequency on the rogue wave profile and on the probability of lingering of the wave in the observation domain. In the last section we conclude our work and summarize future research tasks.

## II. NONLINEAR SCHRÖDINGER EQUATION AND ZENO EFFECT

The quantum mechanics of atomic particles is generally studied in the frame of the Schrödinger equation [29–31]. Since the linearized Schrödinger equation is commonly used, many important nonlinear phenomena is either unknown or ignored by the researchers working in the field of quantum science. However, in order to study nonlinear phenomena such as rational rogue wave solitons, it is mandatory to utilize NLSE [1]. With this aim, we consider the nondimensional NLSE given as

$$i\psi_t + \frac{1}{2}\psi_{xx} + |\psi|^2\psi = 0 \quad (1)$$

where  $x, t$  are the spatial and temporal variables,  $i$  is the complex number and  $\psi$  is the complex amplitude known as the wavefunction. This notation is mainly used in quantum mechanics and hydrodynamics whereas  $t$  and  $x$  axes are switched in fiber optics studies, where NLSE is used to describe the dynamics of light pulses in nonlinear fiber optical media.

It is known that the NLSE given by Eq.(1) admits many different types of analytical solutions. Some of these solutions are reviewed in the next section of this paper. For arbitrary wavefunctions, where the analytical solution is unknown, the NLSE can be numerically solved by a split-step Fourier method (SSFM), which is one of the most commonly used forms of the spectral methods. Similar to other spectral methods, the spatial derivatives are calculated using spectral techniques in SSFM. Some applications of the spectral techniques can be seen in [32–46] and their more comprehensive analysis can be seen in [47, 48].

The temporal derivatives in the governing equations is calculated using time integration schemes such as Adams-Bashforth and Runge-Kutta etc. [37, 47, 48], however SSFM uses an exponential time stepping function for this purpose. SSFM is based on the idea of splitting the equation into two parts, namely the linear and the nonlinear parts. Then time stepping is performed starting from the initial conditions. In a possible splitting we take the first part of the NLSE as

$$i\psi_t = -|\psi|^2\psi \quad (2)$$

which can exactly be solved as

$$\tilde{\psi}(x, t_0 + \Delta t) = e^{i|\psi(x, t_0)|^2\Delta t} \psi_0 \quad (3)$$

where  $\Delta t$  is the time step and  $\psi_0 = \psi(x, t_0)$  is the initial condition. The second part of the NLSE can be written as

$$i\psi_t = -\frac{1}{2}\psi_{xx} \quad (4)$$

Using a Fourier series expansion we obtain

$$\psi(x, t_0 + \Delta t) = F^{-1} \left[ e^{-ik^2/2\Delta t} F[\tilde{\psi}(x, t_0 + \Delta t)] \right] \quad (5)$$

where  $k$  is the wavenumber. Combining Eq.(3) and Eq.(5), the final form of the SSFM becomes

$$\psi(x, t_0 + \Delta t) = F^{-1} \left[ e^{-ik^2/2\Delta t} F[e^{i|\psi(x, t_0)|^2\Delta t} \psi_0] \right]. \quad (6)$$

Starting from the initial conditions, the time integration of the NLSE can be done by the SSFM. Two fast Fourier transform (FFT) operations per time step are needed for this form of the SSFM. The time step is selected as  $\Delta t = 10^{-3}$ , which does not cause a stability problem. The number of spectral components are taken as  $M = 2048$  in order to use the FFT routines efficiently.

Although it is known that the decay of an atomic particle can be inhibited by Zeno dynamics, it remains an open question whether the rogue waves in the quantized optical fields and rogue wavefunctions of the evolving atomic particles in the frame of the NLSE can be stopped by Zeno dynamics. In this paper we analyze the Zeno dynamics of such rogue waves by using the SSFM reviewed above. Although analytical solution of the NLSE is known and used as initial conditions in time stepping of SSFM, after a positive Zeno measurement the wavefunction becomes complicated thus numerical solution is needed. Quantum Zeno dynamics is generally modeled by some operations on the density matrix or Hamiltonian of a quantum system [8–10]. Recently a theoretical wavefunction formulation of the quantum Zeno dynamics is proposed in [49], used in [50, 51] and experimentally tested in [52]. In this formulation after a positive measurement the particle is found in the observation domain of  $[-L, L]$  with a probability of  $\psi_T(x, t) = \psi(x, t)\text{rect}(x/L)/\sqrt{P}$  where  $P = \int_{-L}^L |\psi(x, t)|^2 dx$  and  $\text{rect}(x/L) = 1$  for  $-L \leq x \leq L$ , 0 elsewhere [49]. Between two successive positive measurements, the wave evolves according to NLSE. This cycle can be summarized as

$$\begin{aligned} \psi_T \left( x, \frac{(n-1)t}{N} \right) &\xrightarrow{\text{evolve}} \psi \left( x, \frac{nt}{N} \right) \xrightarrow{\text{measure}} \\ \psi_T \left( x, \frac{nt}{N} \right) &= \psi \left( x, \frac{nt}{N} \right) \frac{\text{rect}(x/L)}{\sqrt{P_N^n}} \end{aligned} \quad (7)$$

where  $n$  is the observation index,  $N$  is the number of observations [49] and

$$P_N^n = \int_{-L}^L \left| \psi \left( x, \frac{nt}{N} \right) \right|^2 dx \quad (8)$$

The cumulative probability of finding the wave in the observation domain becomes [49]

$$P_N = \prod_{n=1}^N P_N^n \quad (9)$$

Using the momentum representation of the linearized Schrödinger equation and analogy of optical wave dynamics of Fabry-Perot resonator, an analytical derivation

of the lingering probability of an atomic particle in the interval of  $[-L, L]$  after  $n^{\text{th}}$  measurement is given as

$$P_N^n \approx 1 - 0.12 \left(\frac{4}{\pi}\right)^2 \left(\frac{2\pi t}{N}\right)^{3/2} \quad (10)$$

in [49]. After  $N$  measurements the cumulative probability of finding the particle in the observation domain becomes

$$P_N \approx \left(1 - 0.12 \left(\frac{4}{\pi}\right)^2 \left(\frac{2\pi t}{N}\right)^{3/2}\right)^N \quad (11)$$

which can further be simplified using Newton's binomial theorem [49]. The reader is referred to [49] for the details of the derivation of these relations. We compare the analytical relations given in Eqs.(10)-(11) with the numerical probability calculations in the next section of this paper.

### III. RESULTS AND DISCUSSION

#### A. Freezing Akhmediev Breathers

In order to study the Zeno dynamics of rogue waves we first consider the Akhmediev breather (AB) solution of the NLSE given in Eq.(1). It is known that the NLSE admits a solution in the form of

$$\psi_{AB} = \left[1 + \frac{2(1-2a) \cosh(bt) + ib \sinh(bt)}{\sqrt{2a} \cos(\lambda t) - \cosh(bt)}\right] \exp[it] \quad (12)$$

where  $a$  is a free parameter,  $\lambda = 2\sqrt{1-2a}$  and  $b = \sqrt{8a(1-2a)}$  [53, 54]. This solution is known as AB and plays an essential role in describing the modulation instability mechanism and rogue wave generation. Experiments have demonstrated that the ABs can exist in optical fibers [54]. The triangularization of the Fourier spectrum, i.e. the triangular supercontinuum generation, plays a key role in the generation and early detection mechanisms of rogue waves. Thus, we also examine the spectra of ABs under quantum Zeno effect.

In Fig. 1, 3D plots of the AB for  $a = 0.45$  and its Fourier spectrum are depicted in the first row. This AB is freely evolving for the time interval of  $t = [-5, 5]$ . In the second row of Fig. 1, we present the AB under Zeno effect and its Fourier spectrum. This AB evolved freely in the time interval of  $t = [-5, 0]$  and it was continuously subjected to Zeno observations in the time interval of  $t = [0, 5]$  within  $L = [-15, 15]$ . For a better visualization of the effect of Zeno observations, the wavefunction is not normalized in this figure.

Next we apply the similar procedure to the AB, but with a narrower region of observation which is selected as  $L = [-5, 5]$  to illustrate the effects of narrowing the observation domain as depicted in Fig. 2. Due to Fourier duality principle, the AB frozen in this fashion has a

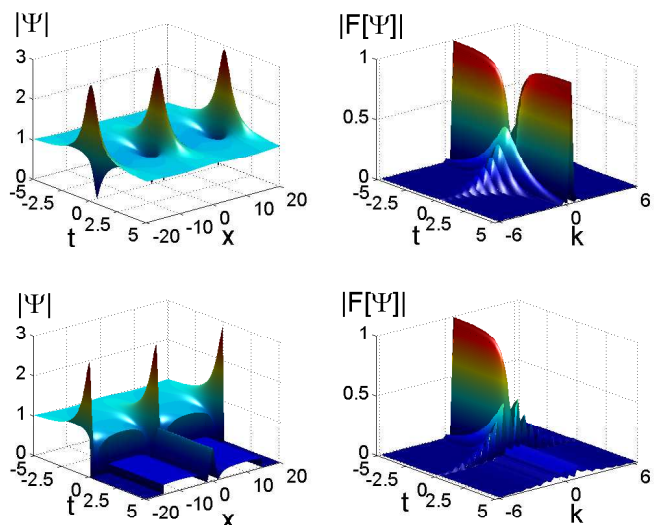


FIG. 1: Quantum Zeno dynamics of an Akhmediev breather with  $a = 0.45$  a) freely evolving wavefunction b) its Fourier spectrum c) continuously observed Akhmediev breather in  $[-15, 15]$  during  $t = [0 - 5]$  d) its Fourier spectrum.

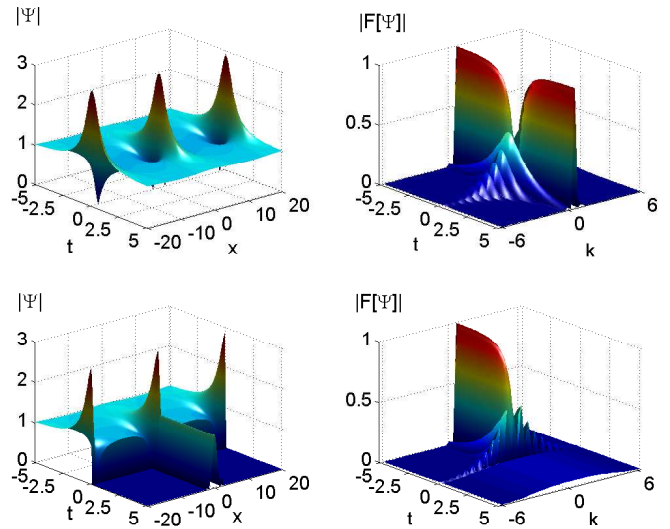


FIG. 2: Quantum Zeno dynamics of an Akhmediev breather with  $a = 0.45$  a) freely evolving wavefunction b) its Fourier spectrum c) continuously observed Akhmediev breather in  $[-5, 5]$  during  $t = [0 - 5]$  d) its Fourier spectrum.

wider spectrum compared to its counterpart presented in Fig. 1.

Depending on the width of the Zeno observation domain, it is possible to freeze the whole AB wavefunction and thus its triangular spectrum during the observation time.

## B. Freezing Peregrine Soliton

Rogue waves of the NLSE is considered to be in the form of rational soliton solutions [1]. The simplest rational soliton solution of the NLSE is the Peregrine soliton [55, 56]. It is given by

$$\psi_1 = \left[ 1 - 4 \frac{1 + 2it}{1 + 4x^2 + 4t^2} \right] \exp[it] \quad (13)$$

where  $t$  and  $x$  denote the time and space, respectively [1]. This solution can be recovered as the limiting case of the AB when the period of the solution tends to infinity. It has been shown that Peregrine soliton is only a first order rational soliton solution of the NLSE [1]. Higher order rational soliton solutions of the NLSE and a hierarchy of obtaining those rational solitons based on Darboux transformations are given in [1]. Throughout many simulations [1, 3, 4] and some experiments [56], it has been confirmed that rogue waves can be in the form of the first (Peregrine) and higher order rational soliton solutions of the NLSE.

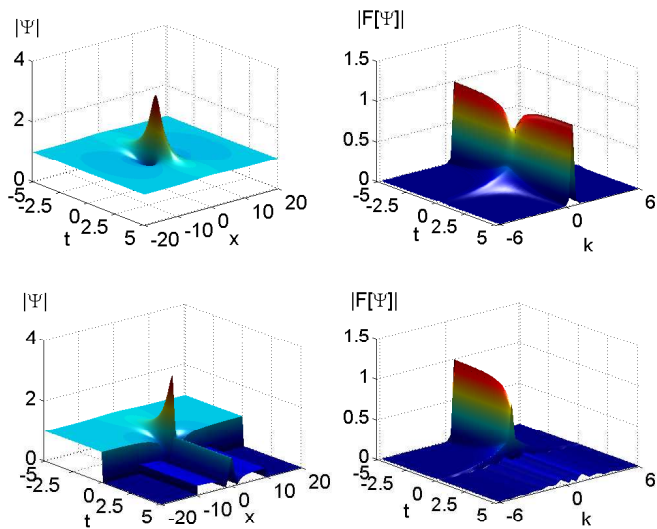


FIG. 3: Quantum Zeno dynamics of a Peregrine soliton a) freely evolving wavefunction b) its Fourier spectrum c) continuously observed Peregrine soliton in the interval of  $[-5, 5]$  during  $t = [0 - 5]$  d) its Fourier spectrum.

Similar to the AB case, in order to analyze the Zeno dynamics of the Peregrine soliton we apply the procedure described by Eqs.(7)-(9). In Fig. 3, plots of the Peregrine soliton and its Fourier spectrum are shown in the first row. This Peregrine soliton evolved freely during the time interval of  $t = [-5, 5]$ . In the second row of Fig. 3, we present the Peregrine soliton inhibited by Zeno observations and its corresponding Fourier spectrum. In this plot the Peregrine soliton evolved freely during the temporal interval of  $t = [-5, 0]$  and it was continuously subjected to Zeno observations in the time interval of

$t = [0, 5]$  within  $L = [-15, 15]$ . For a better visualization of the effect of Zeno observations, the wavefunction is not normalized in this figure as before. Again depending on the width of the Zeno observation domain, it is possible to freeze the Peregrine soliton wholly or partially and thus its triangular spectrum during the observation time.

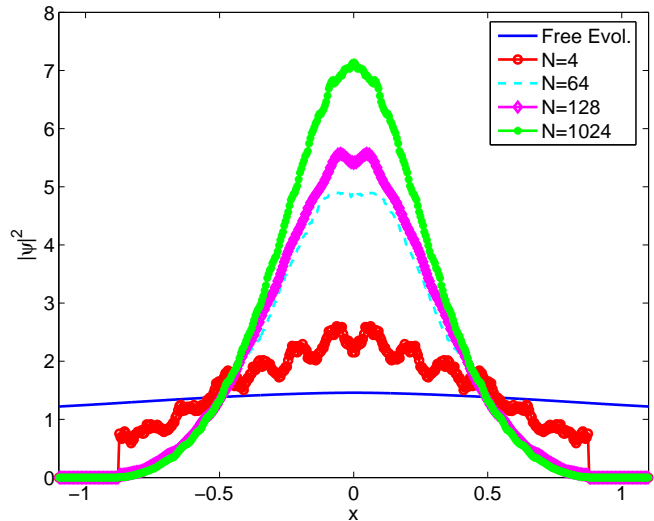


FIG. 4: Probability density (unnormalized) after  $N$  intermediate measurements of the Peregrine soliton in the interval  $[-0.8, 0.8]$  for a time  $t = n/N = 2$ .

In Fig. 4, we present the unnormalized wavefunction with different observation numbers ( $N$ ). For a larger number of intermediate measurements, the decay of Peregrine soliton is inhibited for longer times compared to the case of fewer Zeno observations. This is due to the fact that for a smaller number of observations the evolution time between two successive observations increases. Thus the wavefunction diffuses in this relatively large temporal interval. The constant background level of unity is diminished since the probability vanishes in the unobserved regions of the evolution domain for a positive measurement.

In Fig. 5, we present the normalized probabilities of finding the particle in the observation domain for a time interval of  $t = [0, 2]$ . The dashed lines show the probabilities obtained analytically by Eqs.(10)-(11) whereas the continuous lines represent numerical results. Since the numerical results are obtained using the NLSE and the analytical distributions given by Eqs.(10)-(11) rely on the assumption that the particle's motion is governed by linearized Schrödinger equation, some discrepancies appear between two results, where the discrepancies are less for more frequent observations as expected.

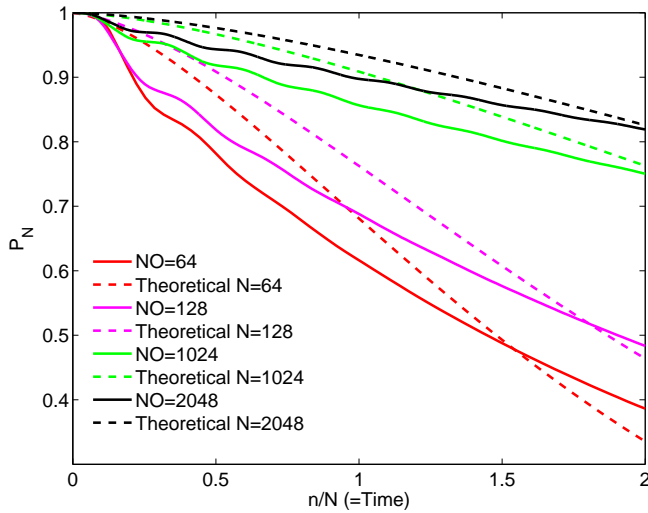


FIG. 5: The probability of finding the Peregrine soliton in the interval  $[-0.8, 0.8]$  for a time of  $t = n/N = 2$  after  $N$  intermediate measurements.

### C. Freezing Akhmediev-Peregrine Soliton

Second order rational soliton solution of the NLSE is Akhmediev-Peregrine soliton [1], which is considered to be a model for rogue waves with higher amplitude than the Peregrine soliton. The formula of Akhmediev-Peregrine soliton is given as

$$\psi_2 = \left[ 1 + \frac{G_2 + itH_2}{D_2} \right] \exp[it] \quad (14)$$

where

$$G_2 = \frac{3}{8} - 3x^2 - 2x^4 - 9t^2 - 10t^4 - 12x^2t^2 \quad (15)$$

$$H_2 = \frac{15}{4} + 6x^2 - 4x^4 - 2t^2 - 4t^4 - 8x^2t^2 \quad (16)$$

and

$$D_2 = \frac{1}{8} \left[ \frac{3}{4} + 9x^2 + 4x^4 + \frac{16}{3}x^6 + 33t^2 + 36t^4 + \frac{16}{3}t^6 - 24x^2t^2 + 16x^4t^2 + 16x^2t^4 \right] \quad (17)$$

where  $t$  is the time and  $x$  is the space parameter [1]. Using Darboux transformation formalism this soliton can be obtained using the Peregrine soliton as the seed solution [1]. Many numerical simulations also confirm that rogue waves in the NLSE framework can also be in the form of Akhmediev-Peregrine soliton [1, 3, 4] however to our best knowledge an experimental verification of this soliton still do not exist.

As in the AB and Peregrine soliton cases, in order to analyze the Zeno dynamics of the Akhmediev-Peregrine

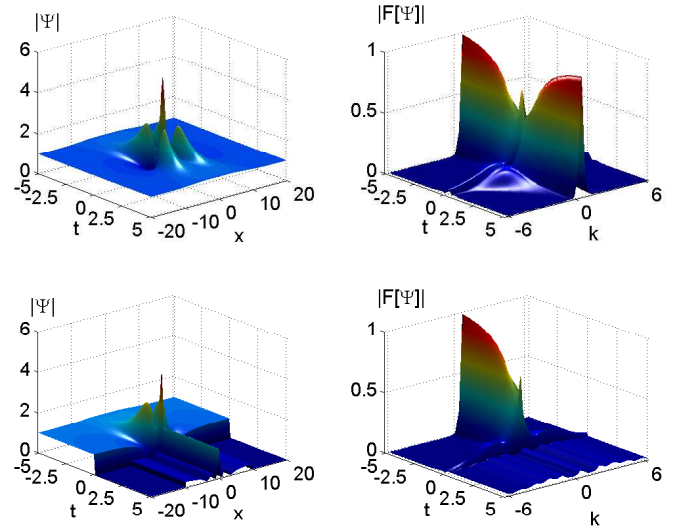


FIG. 6: Quantum Zeno dynamics of an Akhmediev-Peregrine soliton a) freely evolving wavefunction b) its Fourier spectrum c) continuously observed Akhmediev-Peregrine soliton in the interval of  $[-5, 5]$  during  $t = [0, 5]$  d) its Fourier spectrum.

soliton we apply the procedure described by Eqs.(7)-(9). Similarly, in Fig. 6, the Akhmediev-Peregrine soliton, which evolved freely during the time interval of  $t = [-5, 5]$ , and its Fourier spectrum are plotted in the first row. In the second row of Fig. 6, the Akhmediev-Peregrine soliton inhibited by Zeno observations and its corresponding Fourier spectrum are depicted. In this plot the Akhmediev-Peregrine soliton evolved freely during the temporal interval of  $t = [-5, 0]$  and continuous Zeno observations took place time within  $L = [-15, 15]$  during the time interval of  $t = [0, 5]$ .

Again unnormalized wavefunction is depicted in this figure for a better visualization of the effect of Zeno observations on the Akhmediev-Peregrine soliton. Again depending on the width of the Zeno observation domain, it is possible to freeze the Akhmediev-Peregrine soliton wholly or partially and thus its triangular spectrum can be preserved during the observation time.

In Fig. 7, the unnormalized wavefunctions for different observation numbers ( $N$ ) are shown. Similar to the previous cases, for a larger number of intermediate measurements, the decay of Akhmediev-Peregrine soliton is inhibited for longer times compared to the case of fewer Zeno observations due to shorter diffusion time between two positive Zeno observations. Additionally, the peak as well as two dips of the Akhmediev-Peregrine soliton can be preserved during measurements depending on the length of the observation domain. Similarly, since the probability vanishes in the unobserved regions of the evolution domain for a positive measurement, the constant background level of unity is diminishes.

In Fig. 8, we present the normalized probabilities of finding the particle in the observation domain for a time

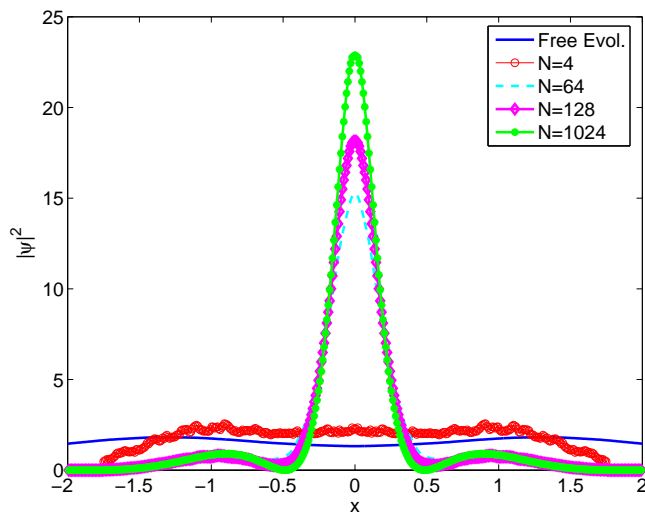


FIG. 7: Probability density after  $N$  intermediate measurements of the Akhmediev-Peregrine soliton in the interval  $[-1.7, 1.7]$  for a time  $t = n/N = 2$ .

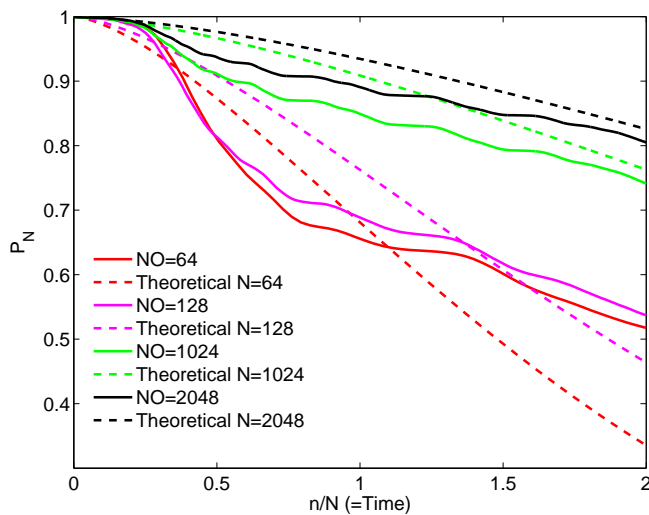


FIG. 8: The probability of finding the Akhmediev-Peregrine soliton in the interval  $[-0.8, 0.8]$  for a time of  $t = n/N = 2$  after  $N$  intermediate measurements.

interval of  $t = [0, 2]$ . The dashed lines show the probabilities obtained analytically by Eqs.(10)-(11) whereas the continuous lines represent numerical results. As before, since the numerical results are obtained using the NLSE and the analytical distributions given by Eqs.(10)-(11) rely on the assumption that the particle's motion is governed by linearized Schrödinger equation, some discrepancies appear between two results, where the discrepan-

cies are less for more frequent observations as expected. However the discrepancies are slight higher compared to the Zeno dynamics of the Peregrine soliton depicted in Fig. 5 due to increased steepness of the Akhmediev-Peregrine soliton.

#### IV. CONCLUSION

In this paper we have numerically investigated the Zeno dynamics of the rogue waves, that appear in the optical and quantum mechanical fields, in the frame of the standard NLSE. Specifically we have analyzed the Zeno dynamics of the Akhmediev breathers, Peregrine and Akhmediev-Peregrine soliton solutions of the NLSE, which are considered as accurate rogue wave models. We have showed that frequent measurements of the rogue wave inhibits its movement in the observation domain for each of these solutions. We have analyzed the spectra of the rogue waves to observe the supercontinuum generation under Zeno observations. Fourier as well as the wavelet spectra of rogue waves under Zeno dynamics may give some clue about the application time (position) of the Zeno observations to freeze the emergence or decay of rogue waves. This would especially be important for the Zeno dynamics of stochastic wavefields which produce rogue waves. We have also analyzed the effect of observation frequency on the rogue wave profile and on the probability of freezing the wave in the observation domain. We have showed that the rogue wave shape can be preserved for longer times and the probability of the freezing the rogue wave increases for more frequent observations, for all three types of rogue waves considered.

The revival dynamics, that is the dynamics after Zeno observations are ceased, of rogue waves will be a part of future work. The analysis of statistical distributions and the shapes of rogue waves in the stochastic fields after Zeno observation remains as a problem which need further attention as well. Using the results presented in this paper and with some future work researchers can model the dynamics of standing and propagating rogue waves observed in the optics and quantum mechanics. More specifically the procedure analyzed in this paper in the frame of the standard NLSE can be used to advance optical and quantum communications and vibrations with special applications which include but are not limited to freezing and steering the rogue and other wave types, avoiding their breaking, imposing a time delay by Zeno effect. The procedure analyzed in this paper in the frame of the standard NLSE can also be extended to model the Zeno dynamics of the many other fascinating nonlinear phenomena which can be used to advance the optical and quantum science and technology.

[1] N. Akhmediev, A. Ankiewicz and J. M. Soto-Crespo, Phys. Rev. E, **80**, 026601 (2009).

[2] C. Bayındır, Phys. Lett. A, **380**, 156 (2016).

- [3] N. Akhmediev, J. M. Soto-Crespo and A. Ankiewicz, *Phys. Lett. A*, **373**, 2137 (2009).
- [4] N. Akhmediev, J. M. Soto-Crespo, A. Ankiewicz and N. Devine, *Phys. Lett. A*, **375**, 2999 (2011).
- [5] D. R. Solli, C. Ropers, P. Koonath and B. Jalali, *Nature*, **450**, 1054 (2007).
- [6] B. Misra and E. C. G. Sudarshan, *J. Math. Phys.* **18**, 756763 (1977).
- [7] P. Facchi and S. Pascazio, *J. Phys. A: Math. Theor.* **41**, 493001 (2008).
- [8] J. M. Raimond, C. Sayrin, S. Gleyzes, I. Dotsenko, M. Brune, S. Haroche, P. Facchi and S. Pascazio, *Phys. Rev. Lett.*, **105**, 213601 (2010).
- [9] J. M. Raimond, P. Facchi, B. Peaudecerf, S. Pascazio, C. Sayrin, I. Dotsenko, S. Gleyzes, M. Brune and S. Haroche, *Phys. Rev. A*, **86**, 032120 (2012).
- [10] A. Signoles, A. Facon, D. Grosso, I. Dotsenko, S. Haroche, J. M. Raimond, M. Brune and S. Gleyzes, *Nat. Phys.*, **10**, 715 (2014).
- [11] L. M. Duan and G. C. Guo, *Phys. Rev. Lett.* **79**, 1953 (1997).
- [12] L. M. Duan and G. C. Guo, *Phys. Rev. A* **57**, 2399 (1998).
- [13] L. Viola and S. Lloyd, *Phys. Rev. A* **58**, 2733 (1998).
- [14] S. Maniscalco, F. Francica, R. L. Zaffino, N. L. Gullo and F. Plastina, *Phys. Rev. Lett.* **100**, 090503 (2008).
- [15] A. Nourmandipour, M. K. Tavassoly and M. A. Bolorizadeh, *J. Opt. Soc. Am. B* **33**, 1723 (2016).
- [16] J. Bernu, S. Deleglise, C. Sayrin, S. Kuhr, I. Dotsenko, M. Brune, J. M. Raimond and S. Haroche, *Phys. Rev. Lett.* **101**, 108402 (2008).
- [17] X. B. Wang, J. Q. You and F. Nori, *Phys. Rev. A* **77**, 062339 (2008).
- [18] S. Bugu, C. Yesilyurt, and F. Ozaydin, *Phys. Rev. A* **87**, 032331 (2013).
- [19] F. Ozaydin, S. Bugu, C. Yesilyurt, A. A. Altintas, M. Tame and S. K. Ozdemir, *Phys. Rev. A* **89**, 042311 (2014).
- [20] C. Yesilyurt, S. Bugu, F. Ozaydin, A. A. Altintas, M. Tame, L. Yang and S. K. Ozdemir, *J. Opt. Soc. Am. B* **33**, 2313 (2016).
- [21] X. P. Zang, M. Yang, F. Ozaydin, W. Song and Z. L. Cao, *Sci. Rep.* **5**, 16245 (2015).
- [22] X. P. Zang, M. Yang, F. Ozaydin, W. Song and Z. L. Cao, *Opt. Exp.* **24**, 12293 (2016).
- [23] Y. H. Chen, B. H. Huang, J. Song, and Y. Xia, *Opt. Comm.* **380**, 140 (2016).
- [24] G. Barontini, L. Hohmann, F. Haas, J. Esteve, and J. Reichel, *Science* **349**, 1317 (2016).
- [25] H. Nakazato, T. Takazawa, and K. Yuasa, *Phys. Rev. Lett.* **90**, 060401 (2008).
- [26] K. Yamane, M. Ito, M. Kitano, *Opt. Comm.* **192**, 299 (2001).
- [27] P. Biagioni, G. Della Valle, M. Ornigotti, M. Finazzi, L. Duo, P. Laporta and S. Longhi, *Opt. Exp.* **16**, 3762 (2008).
- [28] K. T. McCusker, Y. P. Huang, A. S. Kowligy and P. Kumar, *Phys. Rev. Lett.* **110**, 240403 (2013).
- [29] D. J. Griffiths. *An Introduction to Quantum Mechanics*, Prentice Hall, USA (2004).
- [30] L. D. Landau and E. M. Lifschitz. *Quantum mechanics*, Pergamon Press, UK (1958).
- [31] R. H. Fowler and L. Nordheim, *Proc. R. Soc. Lond. A*, **119**, 173 (1928).
- [32] C. Bayındır, MS Thesis, University of Delaware (2009).
- [33] C. Bayındır. arXiv Preprint, arXiv:1604.06604 (2016).
- [34] C. Bayındır. *TWMS J. App. & Eng. Math.*, **6-1**, 135 (2016).
- [35] C. Bayındır, *TWMS J. App. & Eng. Math.*, **5**, 298 (2015).
- [36] C. Bayındır. arXiv Preprint, arXiv:1602.05339 (2016).
- [37] H. Demiray and C. Bayındır, *Phys. of Plasmas*, **22**, 092105 (2015).
- [38] C. Bayındır. arXiv Preprint, arXiv:1602.00816 (2016).
- [39] E. A. Karjadi, M. Badiey and J. T. Kirby, *J. Acoust. Soc. Am.*, **127**, 1787 (2010).
- [40] E. A. Karjadi, M. Badiey, J. T. Kirby and C. Bayındır, *IEEE J. Oceanic Eng.*, **37**, 112 (2012).
- [41] C. Bayındır. arXiv Preprint, arXiv:1512.03932 (2016).
- [42] C. Bayındır, *Sci. Rep.*, **6**, 22100 (2016).
- [43] C. Bayındır. arXiv Preprint, arXiv:1512.03584 (2016).
- [44] C. Bayındır. *Phys. Rev. E*, **93**, 032201 (2016).
- [45] C. Bayındır. *Phys. Rev. E*, **93**, 062215 (2016).
- [46] C. Bayındır. arXiv Preprint, arXiv:1611.08551 (2016).
- [47] C. Canuto. *Spectral Methods: Fundamentals in Single Domains*, Springer-Verlag (2006).
- [48] L. N. Trefethen. *Spectral Methods in MATLAB*, SIAM, Philadelphia (2000).
- [49] M. A. Porras, A. Luis and I. Gonzalo, *Phys. Rev. A*, **90**, 062131 (2014).
- [50] M. A. Porras, I. Gonzalo and A. Luis, *Phys. Rev. A*, **93**, 040101(R) (2016).
- [51] M. A. Porras, A. Luis, I. Gonzalo and A. S. Sanz, *Phys. Rev. A*, **84**, 052109 (2011).
- [52] M. A. Porras, A. Luis and I. Gonzalo, *Phys. Rev. A*, **88**, 052101 (2013).
- [53] N. Akhmediev and V. I. Korneev, *Theor. Math. Phys.*, **69**, 1089 (1986).
- [54] J. M. Dudley, G. Genty, F. Dias, B. Kibler and N. Akhmediev, *Opt. Exp.*, **17**, 21497 (2009).
- [55] D. H. Peregrine, *J. Austral. Math. Soc. B.*, **25**, 16 (1983).
- [56] B. Kibler, J. Fatome, C. Finot, G. Millot, F. Dias, G. Genty, N. Akhmediev and J. M. Dudley, *Nat. Phys.*, **6**, 790 (2010).